Запропоновано нову структуру зарядної станції для електромобілів, що розроблена на базі трифазного трансформатора та тирівневого активного чотириквадрантного випрямляча з корекцією коефіцієнта потужності. Описано параметри запропонованої структури зарядної станції, представлено параметри схеми заміщення акумуляторного відсіку електромобіля Tesla model S, яку приведено до однієї еквівалентної батареї. Описано метод швидкого заряду батареї постійним струмом і постійною напругою CC-CV, при якому забезпечується більша кількість циклів заряду-розряду батареї. Наведено математичні формули для розрахунку складових втрат потужності і ККД запропонованої структури зарядної станції на інтервалі повного заряду батареї.

Представлено систему автоматичного регулювання струму та напруги заряду, яку засновано на широтно-імпульсній модуляції другого роду та інтегральному регуляторі. Представлено імітаційну модель запропонованої структури зарядної станції в програмному середовищі Matlab/Simulink, а також приведено результати моделювання: осцилограми вхідних та вихідних струмів і напруг, наведено динаміку роботи регулятора струму заряду. Шляхом поліноміальної апроксимації енергетичних характеристик IGBT-модулів для розрахунку статичних та динамічних втрат в силових ключах активного випрямляча було створено модель розраховувача втрат.

Показано, що при збільшенні значення струму заряду в режимі CC результуюче інтегральне значення ККД процесу заряду знижується, проте у той же час збільшується коефіцієнт потужності та знижується емісія вищих гармонік. Виконано оптимізацію втрат потужності в запропонованій системі зарядної станції за параметрами мінімуму струму заряду та частоти модуляції в ШІМ.

Виконаний аналіз складових енергії втрат в запропонованій структурі підтвердив її енергоефективність в порівнянні з іншими існуючими структурами. Перевагою запропонованої структури є те, що вона забезпечує покращені показники ККД, коефіцієнту потужності та зниження емісії вищих гармонік струму. Отримані такі показники системи: інтегральне значення ККД повного процесу заряду електромобіля методом CC-CV 95.6 %, коефіцієнт потужності 0.99, коефіцієнт гармонічних спотворень вхідного струму 2.5 %

Ключові слова: активний випрямляч, акумуляторна батарея, зарядна станція електромобіля, коефіцієнт потужності, моделювання

UDC 621.314
DOI: 10.15587/1729-4061.2020.204068

IMPROVING ENERGY INDICATORS OF THE CHARGING STATION FOR ELECTRIC VEHICLES BASED ON A THREE-LEVEL ACTIVE RECTIFIER

O. Plakhtii
PhD, Electronic Engineer*
E-mail: a.plakhtiy1989@gmail.com
V. Nerubatskyi
PhD, Associate Professor**
E-mail: NVP9@i.ua
A. Mashura
Postgraduate Student
Department of Industrial and Biomedical Electronics
National Technical University
«Kharkiv Polytechnic Institute»
Kyrpychova str., 2, Kharkiv, Ukraine, 61002
E-mail: artemmashura94@gmail.com
D. Hordiienko
Postgraduate Student**
E-mail: D.Hordiienko@i.ua
H. Khoruzhevskyi
Constructor Engineer*
E-mail: khoruzhevskyi@gmail.com
*Limited Liability Company «VO OVEN»
Hvardiytsiv-Shyronivtsiv str., 3A,
Kharkiv, Ukraine, 61153
**Department of Electric Power Engineering,
Electrical Engineering and Electromechanics
Ukrainian State University of Railway Transport
Feierbakha sq., 7, Kharkiv, Ukraine, 61050

Received date 14.03.2020
Accepted date 20.05.2020
Published date 23.06.2020

1. Introduction

Every year, electric cars become more popular compared to cars with internal combustion engines. The development of electric vehicles (EV) and charging stations is given significant attention to by researchers and manufacturers [1, 2]. At the same time, it is a relevant issue to improve the indicators of energy efficiency of charging stations, namely, to improve efficiency parameters, the indicators of sinusoidal current consumption, and a power factor.

According to the international standard IEC-62196, there are the following types of charging stations: Mode 1, Mode 2, Mode 3, Mode 4. The regulated parameters of charging stations in line with the standard are given in Table 1.

Among these, the most powerful type of charging station that makes it possible to implement the electric vehicle fast-charging mode is Mode 4 [3]. Therefore, our research is aimed at improving the performance indicators of the Mode 4 charging stations.

Table 1

Parameters of charging stations

Type	Phase quantity	Charge voltage, V	Current type	Charge current, A	Charging station arrangement	Charging station location
Mode 1	1	To 250	AC	To 16	Onboard	Home
	3	To 480				Home
Mode 2	1	To 250		To 32		
	3	To 400				
Mode 3	1	To 250		To 32		Private/Public
	1	To 250		To 70		
	3	To 480		To 63		
Mode 4	3	To 1,000	DC	To 500	External	Public

In addition, at modernization, one of the requirements for charging stations is the possibility of ensuring a double-sided transfer of energy, which corresponds to the «vehicle-grid (V2G)» concept [4, 5].

2. Literature review and problem statement

Publications [6, 7] described the charging stations for electric vehicles containing two stages of electricity conversion, namely an input AC/DC rectifier and an output DC/DC converter of direct current (Fig. 1).

In a given topology, input rectifiers used to create a link of constant voltage. Next, the DC/DC converter enables the adjustment of voltage and current of each single electric vehicle charge over a predefined range. In some cases, the DC/DC converter is also used to ensure the galvanic isolation of an electric vehicle with the grid [8, 9]. A common disadvantage of the examined systems [10, 11] is the concept of a two-step energy conversion, which predetermines the power losses in two converters and, accordingly, a decrease in the efficiency of the charging station [12, 13]. Each of the reported technical solutions has its drawbacks and cannot be considered a complete solution to the existing technical issue.

Paper [14] proposed a transducer for the electric vehicle charging station, whose disadvantage is the efficiency value, which reaches 91 % at maximum. In addition, the reported transducer requires the electromechanic phase splitting, namely, the nine-phase power system, which makes the system more expensive and increases its dimensions.

Work [15] studied the efficiency of a charging station for electric vehicles on the basis of an inductive power transfer converter (ITP). The topology of a given converter is shown in Fig. 2. According to the cited work, the converter efficiency depends on many factors and, at certain intervals of operation, decreases to 45–50 %, which is quite low. In addition, the cited work lacks data on the integrated efficiency value of a full battery charging process in an electric car.

Paper [16] studied the efficiency of a charging station of electric vehicles based on a converter, which consists of a rectifier and a parallel three-channel buck-boost converter (Fig. 3). The disadvantage of this topology is the lack of galvanic isolation of the power supply with a load. In addition, according to the cited paper, the peak value of the converter efficiency is less than 92 %, which is quite low. In addition, there are no data on the integrated efficiency value of a full battery charging process in an electric car.

Work [17] reports a study of the ITP-type converter, whose difference from the transducer reported in [15] is that instead of a diode bridge the fully manageable power transistors are used.

According to the study, the converter efficiency, when using power transistors based on silicon carbide (SiC) and gallium arsenide (GaN), is in the range from 83 to 98 %. It is worth noting that the SiC- and GaN-based transistors are considerably more expensive than classic MOSFET or IGBT transistors. In addition, the cited work lacks data on the integrated efficiency value of a full battery charging process.

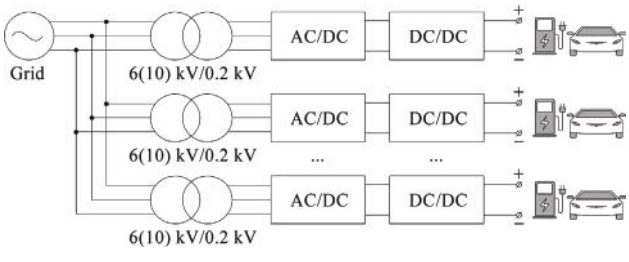

Fig. 1. Circuits of fast-charging stations based on the AC/DC–DC/DC system

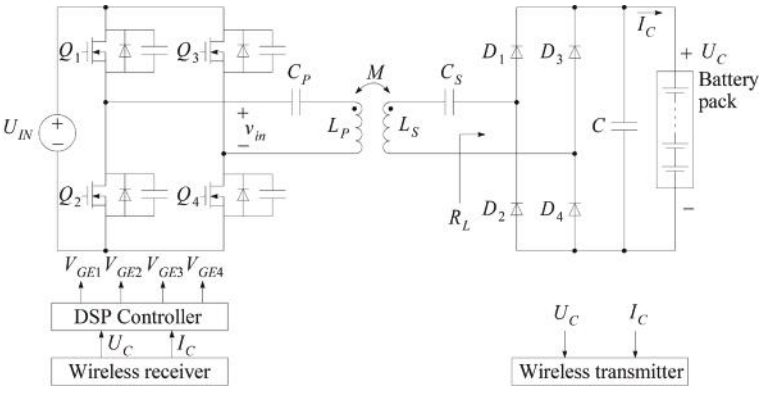

Fig. 2. Inductive power transfer converter

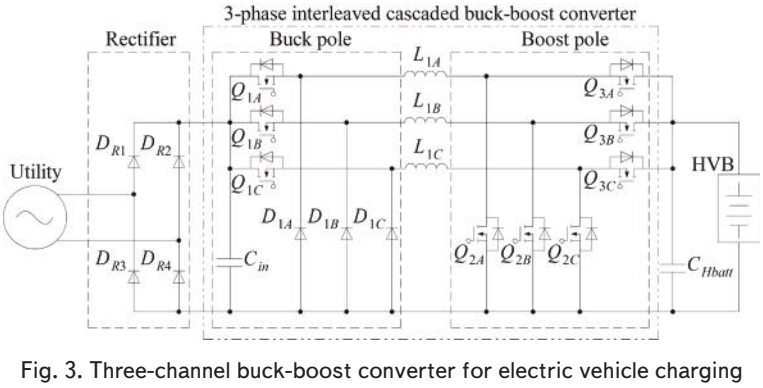

Fig. 3. Three-channel buck-boost converter for electric vehicle charging

Paper [18] reports a study into the half-bridge ITP-type converter, shown in Fig. 4. According to the study, the converter efficiency was determined using an experimental sample with a power of 900 W and reached 92 % to 95.6 %, which is a high enough indicator. However, when charging an electric car with a power of 900 W, the charging process can last more than 90 hours; there are no data on the efficiency of a given converter when implementing a greater power.

Table 2 gives the characteristics of external charging stations [19].

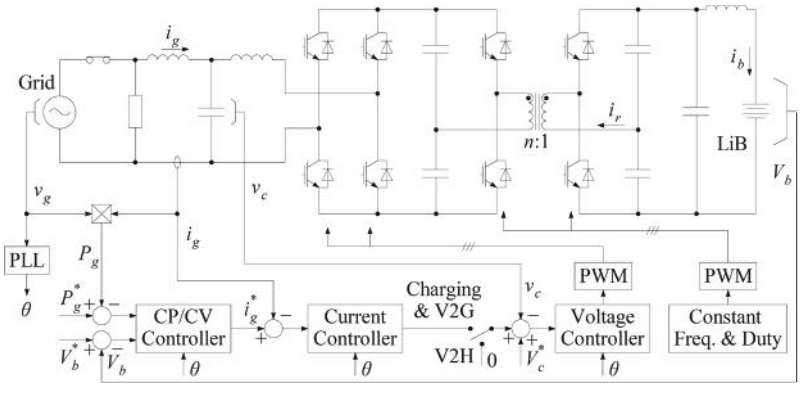

Fig. 4. An electric vehicle charging station based on the half-bridge ITP-type converter

Table 2

Characteristics of external charging stations

Manufacturer and model	ABB Terra 53	Tritium Veefil-RT	Tesla Super-charger	EVTEC espresso&charge
Rated power, kW	50	50	135	150
Charge standard	CCS Type 1 CHAde MO 1.0	CCS Types 1 and 2 CHAde MO 1.0	Super-charger	SAE Combo 1 CHAde MO 1.0
Power voltage	480 VAC	380...480 VAC 600...900 VDC	200...480 VAC	400 VAC±10 %
Direct current output voltage, V	200...500 50...500	200...500 50...500	50...410	170...500
Output direct current, A	120	125	330	300
Efficiency, %	93	>92	92	93

The data in the table show that the efficiency of charging stations does not exceed 93 %.

In addition to the general shortcomings in the examined works, it should be noted that efficiency was estimated in them at the constant value of the charge current while the integrated efficiency value of a charging system over the full interval of charging was not assessed.

Thus, the above review allows us to conclude that it is a relevant task to further improve the energy efficiency of charging stations for electric vehicles. Also of importance is to determine the integrated efficiency value of a full battery charging process in an electric car. Given this, it seems expedient to undertake a study aimed at improving the energy efficiency of charging stations for electric vehicles based on an active three-level rectifier with the power factor correction.

3. The aim and objectives of the study

The aim of this study is to improve the energy indicators of an electric vehicle charging station by using a three-level active rectifier that operates under a power factor correction mode.

To accomplish the aim, the following tasks have been set:

– to introduce the proposed topology of a charging station based on a three-phase transformer and a three-level active rectifier with the power factor correction;

– to outline a procedure for determining the integrated efficiency value of a charging process in the represented system of a charging station for electric vehicles, taking into consideration the parameters of a power grid, the transformer, the converter power switches, and the parameters of an electric car's battery pack compartment;

– to build a simulation model of the proposed charging station in the MATLAB/Simulink programming environment;

– to investigate energy indicators, namely power losses, as well as indicators of electric energy quality in the developed simulation model of a charging station based on a three-level active rectifier.

4. The proposed topology of a charging station

We have proposed the concept of an external direct-current charging station based on an active three-phase rectifier (AR) with the power factor correction (Fig. 5). In this case, the active rectifier performs the function of control over the output voltage and charge current, while the galvanic isolation is enabled by an input transformer.

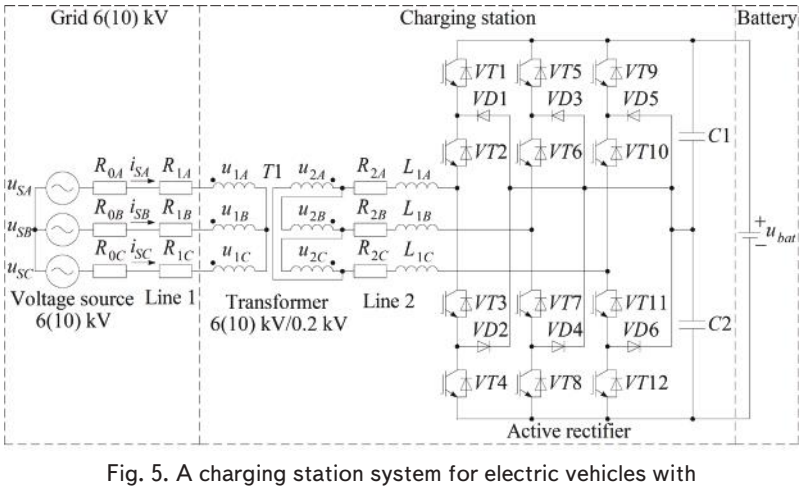

Fig. 5. A charging station system for electric vehicles with a single-stage energy conversion

The advantages of the proposed charging station with AR include:

– the high power ratio, close to unity;

– the low total harmonic distortion coefficient of current consumption (THD<5 %);

– the higher efficiency relative to the two-stage charging stations of the AC/DC– DC/DC type;

– a capacity to provide bilateral energy transfer.

4. 1. Parameters of the proposed charging station

A power grid's characteristics are determined by the parameters of a three-phase power substation transformer of the TMN4000/35/6 type, whose phase resistance is R_{0A}=1.4 Ohm [20, 21]. The line 1 parameters are determined by the distance between the traction substation and the converting transformer, which is accepted equal to 1 km. An aluminum three-wire cable, used in line 1, has a phase resistance magnitude of R_{1A}=0.8 Ohm/km, and its cross-section is selected based on current and is 35 mm^2.

A converting transformer of the SPZ-1000/10UZ 6(10)/0.2 kV series has a nominal power of 0.878 MW and a short-circuit loss of 8 kW [22, 23]. The total equivalent resistance of its phase R_{TV} is 1.73 mOhm. The line 2 parameters are determined by the distance between the converting transformer T1 and the active rectifier, which is taken equal to 50 m. In this case, the cross-section of a copper cable is 350 mm^2, the phase resistance magnitude is R_{2A}=2.5 mOhm. The inductance value of the input valves of the active rectifier is 0.2 mH.

We selected, for the active rectifiers, the switches of the CM600DX-13T type made by Mitsubishi Electric with the parameters of a collector current I_c=600 A and the voltage of a collector-emitter U_{CE}=650 V, the capacity of each output capacitor equals 20 mF. The system of the automated control over the current and voltage of the battery is implemented on the basis of an integrated controller with the subsequent PWM formation of an input current shape [24, 25].

4. 2. The equivalent model of a battery pack

This paper examines the charge of the equivalent model of the battery compartment in the Tesla S electric vehicle, which contains 7,104 batteries by Panasonic NCR-18650b with a total capacity of 85 kWh [26, 27]. The battery connection circuit in the electric vehicle Tesla Model S is shown in Fig. 6.

In the battery compartment, individual batteries of the NCR-18650b type are connected in parallel into groups of 74 pcs. [28, 29]. With a parallel connection, the voltage of the group is equal to the sum of voltages of each element (4.2 V), the capacity of the group is equal to the sum of the capacities of the elements (250 A·h). Next, six groups are connected sequentially into a module.

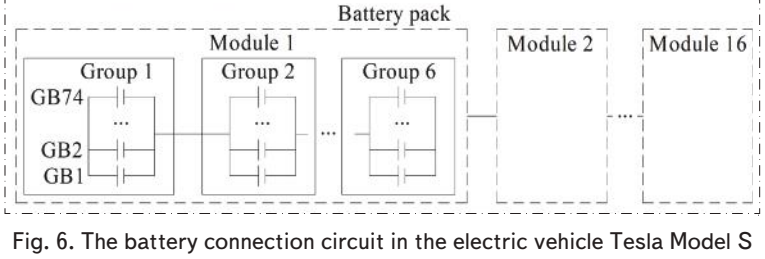

Fig. 6. The battery connection circuit in the electric vehicle Tesla Model S

In this case, the module voltage is summed up with the voltages of the groups and is equal to 25.2 V. The modules are then connected sequentially in a battery. In total, the battery contains 16 modules (96 groups in total). In this case, the voltage of all modules is summed up and is 400 V. We also calculated the equivalent resistance of the battery pack; based on that the average resistance of one rechargeable battery R_{NCR}=37 mOhm is equivalent to the battery resistance R_{bat}=27 mOhm.

4. 3. A battery charging algorithm

When implementing a fast battery charge, a significant role belongs to the method (algorithm), which would be used to charge the battery. The most popular method of battery charging is a Constant Current–Constant Voltage (CV-CV) method (Fig. 7) [30, 31].

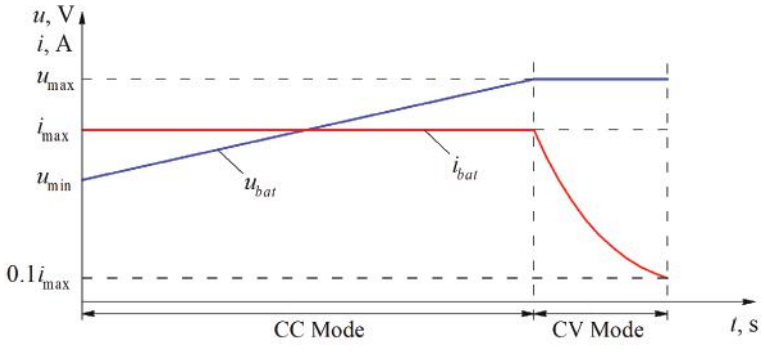

Fig. 7. Charging mode based on a CC-CV method

The main idea of the method is that the battery is charged with the constant maximum current (i_{max}), which is determined by a battery manufacturer to a certain cutoff voltage (u_{max}), then it is charged at this voltage as long as the current consumption is reduced to about 0.1 or less, thereby ensuring a full charge. It should be noted that when switching from a CC mode to a CV mode (this occurs at about 80 % of the battery charge) the charging speed is significantly reduced [32, 33].

5. Calculation of the efficiency and losses of a charging station system

This paper estimated the efficiency of the proposed charging station, shown in Fig. 5. The efficiency was estimated based on the total energy of losses and usable power obtained by a battery over the full charging interval [34]. The efficiency is calculated from the following expression [35]:

$$\eta = \frac{E_{Load}}{E_{Load} + \Delta E_{\Sigma}}, \quad (1)$$

where E_{Load} is the usable energy transmitted to a battery over the charge duration; ΔE_{Σ} is the total energy of losses in the considered micro-grid system.

$$\Delta E_{\Sigma} = E_S + E_{L1} + E_{TV} + E_{L2} + \\ + E_{LR} + E_{AR} + E_{CR} + E_{bat}, \quad (2)$$

where E_S is the energy of losses in a source of 6(10) kV; E_{L1} is the energy of losses in line 1;

E_{TV} is the energy of losses in a transformer; E_{L2} is the energy of losses in line 2; E_{LR} is the energy of losses in input inductances; E_{AR} is the energy of losses in the switches of an active rectifier; E_{CR} is the energy of losses in output capacitors; E_{bat} is the energy of losses in a battery.

The usable energy transmitted to the load:

$$E_{Load} = \int_0^{T_{ch}} \left(u_{Load} \cdot i_{Load}\right) \cdot \mathrm{d}t, \quad (3)$$

where T_{ch} is the full battery EV charge duration; u_{load} is the instantaneous value of the output voltage fed to the lithium-ion battery compartment (when charging, the range varies from 340 to 420 V); i_{load} is the instantaneous value of the load current (a battery charge), which, during charging, varies from 15 to 400 A.

The losses in a source of 6(10) kV, in line 1, in the transformer $T1$, in line 2, and in a battery are calculated from the following formula [36]:

$$E = \int_0^{T_{ch}} \left(i^2 \cdot R\right) \cdot \mathrm{d}t, \quad (4)$$

where i is the instantaneous current value in the section of the calculated circle; R is the instantaneous resistance value in the section of the calculated circle.

The selected switches for the active rectifier were an IGBT-module, the type of CM600DX-13T. The total losses in an IGBT-module consist of the dynamic and static losses in an IGBT-transistor and a reverse diode, calculated from the following expressions [37, 38]:

$$E_{loss.IGBT} = E_{loss.VT} + E_{loss.VD}; \quad (5)$$

$$E_{lossVT} = E_{VT.DC} + E_{VT.SW}; \quad (6)$$

$$E_{lossVD} = E_{VD.DC} + E_{VD.SW}, \quad (7)$$

where $E_{VT.DC}$ is the energy of static losses in IGBT-transistors; $E_{VT.SW}$ is the energy of dynamic losses in IGBT-transistors; $E_{VD.DC}$ is the energy of static losses in parallel diodes; $E_{VD.SW}$ is the energy of dynamic losses in parallel diodes.

$$E_{VT.DC} = \int_0^{T_{ch}} \left(i_c \cdot u_{ce}\right) \mathrm{d}t, \quad (8)$$

where i_c is the collector current; $u_{ce}(i_c)$ is the voltage between a collector and an emitter, which depends on the collector current magnitude. Dynamic losses in IGBT-transistors are determined from the following expression [39]:

$$E_{VT.SW} = \int_0^{T_{ch}} \left[E_{on}\left(I_c\right) + E_{off}\left(I_c\right)\right] \mathrm{d}t, \quad (9)$$

where $E_{on}(I_c)$ is the energy dissipated in a transistor when switching, which depends on the magnitude of a collector's current; $E_{off}(I_c)$ is the energy that dissipates in a transistor at disabling, which depends on the collector's current magnitude.

Static losses in reverse diodes are determined from the following expression [40]:

$$E_{VD.DC} = \int_0^{T_{ch}} \left(u_{fwd} \cdot i_{vd}\right) \mathrm{d}t, \quad (10)$$

where u_{fwd} is the drop in voltage on a reverse diode; i_{vd} is the reverse diode current.

Dynamic losses in reverse diodes are determined from the following expression [41]:

$$E_{VD.SW} = \int_0^{T_{ch}} E_{rec}\left(i_{vd}\right) \mathrm{d}t, \quad (11)$$

where E_{rec} is the reverse diode recovery energy.

Data on $E_{on}(i_c)$, $E_{off}(i_c)$ and $E_{rec}(i_c)$, $u_{ce}(i_c)$, $u_{fwd}(i_{vd})$ are borrowed from a datasheet to the CM600DX-13T module.

6. A simulation model of the proposed charging station

To experimentally test the theoretical assumptions, we built a model of the proposed charging station in the MATLAB programming environment (Fig. 8).

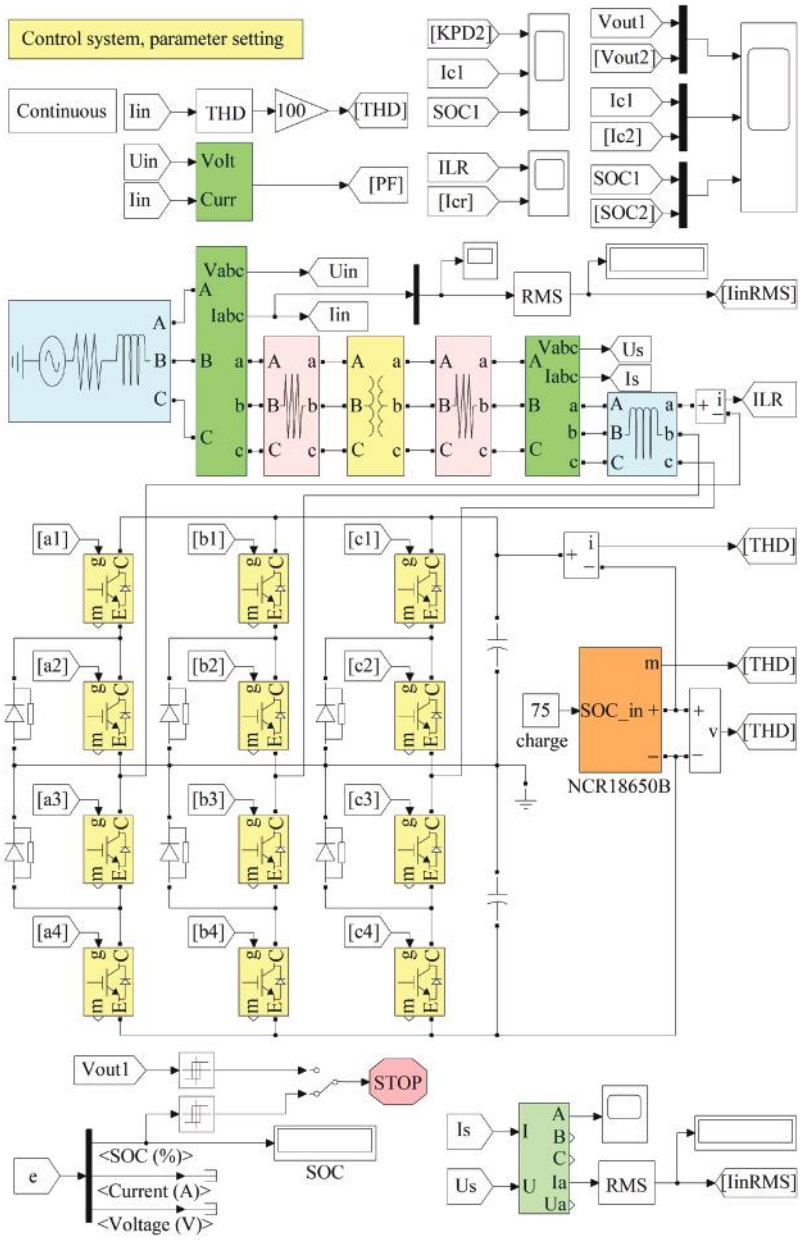

Fig. 8. A MATLAB-model of the micro-grid system of the charging station for electric vehicles

The method for solving differential equations ODE15S (Runge-Kutta method) was applied in simulation modeling, with the permissible relative modeling error of 0.01 %.

The automated control system (ACS) for the active rectifier was built on the basis of an integrated regulator with the subsequent pulse-width modulation [42, 43]. The designed ACS ensures the predefined dynamics of change in the charging voltage and current under the CC-CV modes.

The advantage of a pulse-width modulation method over hysteresis is the possibility of reducing the switching frequency of AR switches; it predetermines the reduction of dynamic losses in the switches and an increase in efficiency [44, 45]. The proposed structural diagram of the AR control system with a pulse-width modulation is shown in Fig. 9, where I_{as}, I_{out}, U_{as}, U_{out} are the currents and voltages of battery charging, received in the feedback and in a job signal unit, respectively.

In the system of automatic regulation of voltage and current of a charge of the battery in the CC-CV mode the integrated regulator is realized. A special feature of the developed controller is that various integrated coefficients are used for setting the current and voltage modes, which improves the dynamics of control in comparison to when the CC and CV modes apply the same coefficient (Fig. 10).

The basic MATLAB models of IGBT-transistors and power diodes do not take into consideration dynamic power losses [46]. In addition, the volt-ampere characteristics of transistors in MATLAB are represented by a linear function, which causes a rather large error in the simulation of static losses. More details about the simulation of static and dynamic losses in the power switches of converters when using the methods of approximation of energy characteristics of transistors are given in ref. [47]. To obtain higher accuracy, we built a model of the counter that takes into consideration all losses in the IGBT-transistors and reverse diodes in the CM600DX-13T module (Fig. 11).

It should be noted that the specified topology of a charging station converter could also be used with alternative power sources, such as solar panels with power storages [48].

The simulation of losses in the IGBT-modules involved the polynomial approximation of graphic dependences $E_{on}(i_c)$, $E_{off}(i_c)$ andi $E_{rec}(i_{vd})$, $u_{ce}(i_c)$, $u_{fwd}(i_{vd})$, which are given in datasheet (the IGBT module CM600DX-13T). The approximation results are given in the following expressions:

$$E_{on}(i_c) = 6.230414 \cdot 10^{-6} \cdot i_c^2 + \\ + 7.992571096 \cdot 10^{-3} \cdot i_c + 1.495824769248; \quad (12)$$

$$E_{off}(i_c) = 39.857 \cdot 10^{-9} \cdot i_c^3 - 55.3643 \cdot 10^{-6} \cdot i_c^2 + \\ + 71.5372 \cdot 10^{-3} \cdot i_c + 2.97379; \quad (13)$$

$$E_{rec}(i_{vd}) = 39.776 \cdot 10^{-9} \cdot i_{vd}^3 - 94.602431 \cdot 10^{-6} \cdot i_{vd}^2 + \\ + 81.874 \cdot 10^{-9} \cdot i_{vd} + 1.2314; \quad (14)$$

$$u_{ce}(i_c) = 0.8639 \cdot i_c^3 - 2.1104 \cdot i_c^2 + \\ + 2.363 \cdot i_c + 0.5114; \quad (15)$$

$$u_{fwd}(i_{vd}) = 1.2433 \cdot i_{vd}^3 - 3.0339 \cdot i_{vd}^2 + \\ + 2.9754 \cdot i_{vd} + 0.5624. \quad (16)$$

We verified the results of calculating losses in IGBT-modules, obtained in MATLAB modeling, using the software MelcoSim 5.1 made by Mitsubishi Electric. Error in the calculation is 2...3 %.

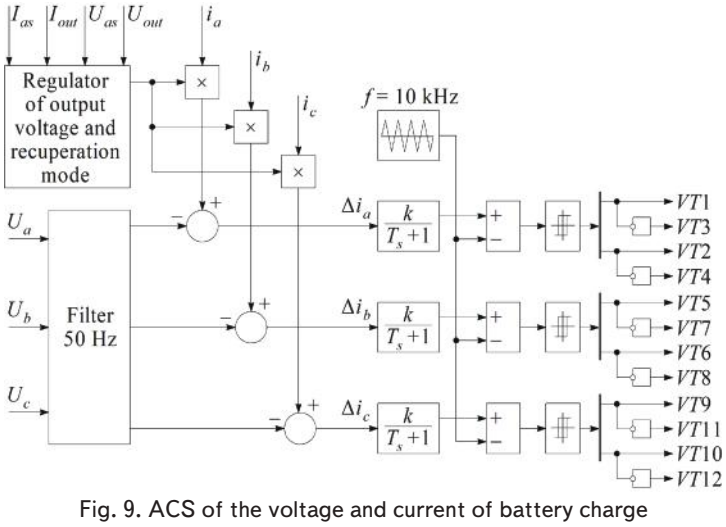

Fig. 9. ACS of the voltage and current of battery charge in a three-phase AR with PWM

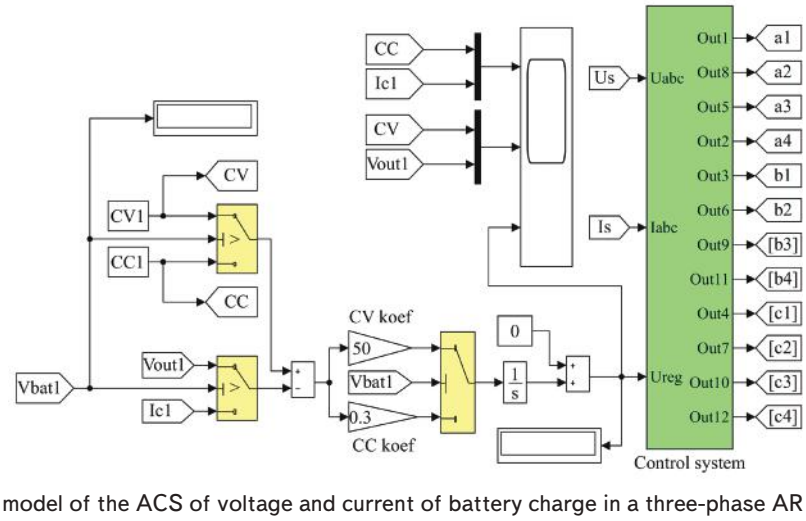

Fig. 10. A model of the ACS of voltage and current of battery charge in a three-phase AR with PWM

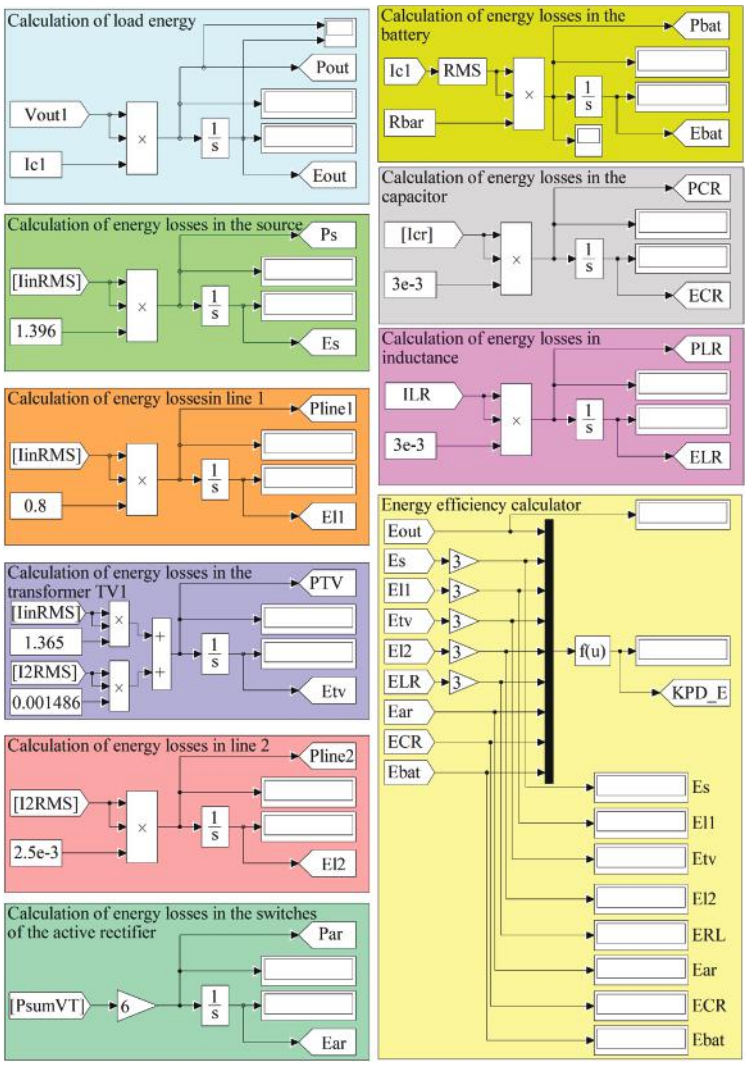

Fig. 11. A MATLAB model of the loss counter in IGBT-modules

7. Investigating energy indicators of the proposed charging station by simulation

The simulation results, namely the oscillographs of the input current and the input voltage of an active rectifier, are shown in Fig. 12.

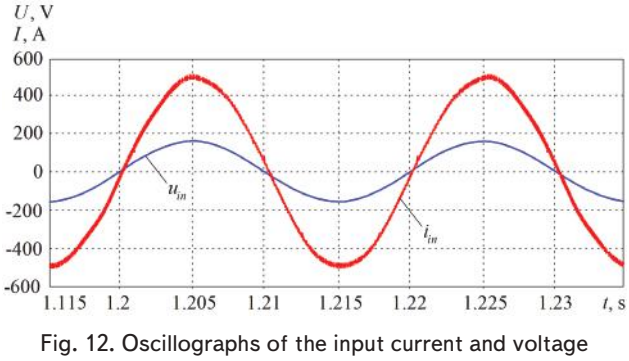

Fig. 12. Oscillographs of the input current and voltage of an active rectifier

The charging process, namely the dynamics of change in the output voltage and current of battery charge, as well as the SOC magnitude of the battery over the entire charging interval, is shown in Fig. 13.

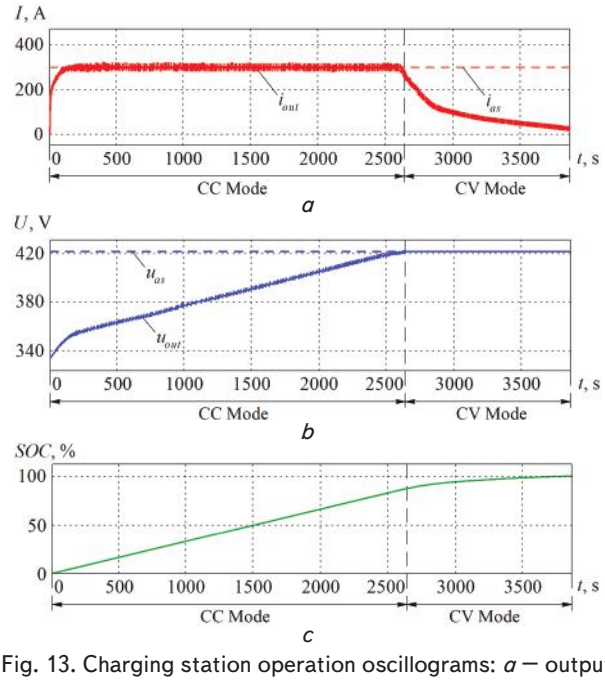

Fig. 13. Charging station operation oscillograms: *a* — output current and setting current (CC); *b* — output voltage and setting voltage (CV); *c* — battery charge level

The result of modeling is the derived values of the efficiency parameters and the components of the energy of losses within the system sections (Table 3).

Table 3

Distribution of losses in the system of a charging station

Components of energy of losses	Energy of losses, W·s	
	f_{PWM}=10 kHz	f_{PWM}=20 kHz
In a source, E_S	1,768	1,761
In line 1, E_{L1}	1,013	1,009
In a transformer, E_{T1}	3,313	3,299
In line 2, E_{L2}	2,664	2,653
In AR input inductors, E_{LR}	3,206	3,192
In AR switches, E_{AR}	7,000	7,913
In output capacitors, E_{CR}	468	464
In a battery, E_{bat}	6,753	6,743
Total losses, ΔE_{Σ}	26,185	27,034

Table 4 gives the values of efficiency, the power factor, and the coefficient of harmonic distortions in a charging station system at different charge currents and the frequency of PWM.

Table 4

Energy parameters of the charging station

PWM frequency, kHz	Charge current under a CC mode, A	Efficiency, %	Charging time, s,·10^3	Power factor	THD, %
5	150 (0.6C)	95.6	6.55	0.985	11.8
	200 (0.8C)	94.8	5.18	0.987	9.8
	250 (1C)	93.9	4.38	0.989	7.2
	300 (1.2C)	93.1	3.84	0.991	6.0
	350 (1.4C)	92.2	3.47	0.992	5.1
	400 (1.6C)	91.4	3.2	0.992	4.5
10	150 (0.6C)	95.4	6.55	0.987	6.1
	200 (0.8C)	94.5	5.19	0.99	4.6
	250 (1C)	93.7	4.38	0.991	3.7
	300 (1.2C)	92.9	3.85	0.992	3.1
	350 (1.4C)	92.1	3.48	0.992	2.7
	400 (1.6C)	91.3	3.2	0.993	2.5

Our research shows that the efficiency of the proposed structure of the charging station is quite high. There is a clearly noticeable dynamics indicating that the higher the charge current, the less the efficiency.

8. Discussion of results of studying the proposed charging station system

The structure of a charging station based on an active three-level rectifier has been suggested in this paper. The proposed technical solution makes it possible to control the charge current and voltage; relative to known technical solutions for charging stations, it provides for the improvements in the efficiency, the power factor, and total harmonic distortion coefficient of charging stations for electric vehicles (Table 4). The efficiency of the charging station, taking into consideration the losses of power in the battery of an electric vehicle at a charge current of 150 A, is 95.6 %, the power factor (PF) of the charging station is in the range of 98.5 % to 99.3 %; total harmonic distortion coefficient lies in the range from 2.5 % to 11.8 %. Such results are explained by the fact that the proposed charging station executes the charging of electric vehicles by a single-stage conversion of electricity with an active three-phase three-level four-quadrant rectifier, which also enables the power factor correction mode.

We have given a procedure for determining the integrated efficiency value of a full charging process in the reported system of a charging station for electric vehicles, taking into consideration the parameters of a power grid, transformer, power switches of the converter, and the parameters of a battery compartment in an electric vehicle. A special feature of the study is a rather precise determination of static and dynamic losses in the power IGBT modules of an active rectifier in a charging station, which was performed using the polynomial approximation of energy characteristics $E_{on}(i_c)$, $E_{off}(i_c)$ and $E_{rec}(i_{vd})$, $u_{ce}(i_c)$, $u_{fwd}(i_{vd})$ – equations (12) to (16). Thus, the calculation of loss takes into consideration the peculiarities of the applied modulation algorithm, as well as all transient processes at charging.

We have given the developed simulation model of the charging station and the results of modeling, which confirmed the high energy indexes of the proposed system.

The limitation of the current study is that the designed simulation model works adequately only under operating modes while under emergency regimes, when the voltage and current values exceed the rated values, the model could prove inadequate.

The disadvantages of the study are the lack of stability analysis of the automated control system.

In further studies, it would be advisable to conduct physical experiments.

9. Conclusions

1. We have proposed the structure of a charging station for electric vehicles consisting of an input transformer, a three-level active rectifier, and a load (the equivalent model of a lithium-ion battery pack in the electric vehicle Tesla Model S), which ensures, relative to known technical solutions for charging stations, the improvements in efficiency, power factor, and total harmonic distortion coefficient. The results obtained are explained by that the proposed charging station implements a one-stage conversion of electricity in an active rectifier with the power factor correction.

2. The procedure has been given and the efficiency of the charging process in the considered system has been calculated. At different parameters of the charge current and the switching frequency, the charging station efficiency, taking into consideration the losses of power in the electric vehicle battery, lies between 91.3 % and 95.6 %.

3. The MATLAB 2017b programming environment has been used to build a simulation model of the proposed charging station. Our study into the energy performance of the charging station based on a three-level active rectifier has shown that the power factor of the charging station lies in the range from 98.5 % to 99.3 %. Total harmonic distortion coefficient in the process of charging is between 2.5 % and 11.8 %.

References

1. Weiss, M., Zerfass, A., Helmers, E. (2019). Fully electric and plug-in hybrid cars – An analysis of learning rates, user costs, and costs for mitigating CO_2 and air pollutant emissions. Journal of Cleaner Production, 212, 1478–1489. doi: https://doi.org/10.1016/j.jclepro.2018.12.019
2. Dai, P., Guo, G., Gong, Z. (2016). A Selection Precharge Method for Modular Multilevel Converter. International Journal of Control and Automation, 9 (4), 161–170. doi: https://doi.org/10.14257/ijca.2016.9.4.16
3. Haq, G., Weiss, M. (2018). Time preference and consumer discount rates - Insights for accelerating the adoption of efficient energy and transport technologies. Technological Forecasting and Social Change, 137, 76–88. doi: https://doi.org/10.1016/j.techfore.2018.06.045
4. Hardman, S., Chandan, A., Tal, G., Turrentine, T. (2017). The effectiveness of financial purchase incentives for battery electric vehicles – A review of the evidence. Renewable and Sustainable Energy Reviews, 80, 1100–1111. doi: https://doi.org/10.1016/j.rser.2017.05.255
5. Lévay, P. Z., Drossinos, Y., Thiel, C. (2017). The effect of fiscal incentives on market penetration of electric vehicles: A pairwise comparison of total cost of ownership. Energy Policy, 105, 524–533. doi: https://doi.org/10.1016/j.enpol.2017.02.054
6. Luo, S., Wang, Q., Lu, S. (2019). A Novel Efficient Electric Vehicle Fast Charging System Structure with Low Order Harmonic Current Suppression Capability. 2019 14th IEEE Conference on Industrial Electronics and Applications (ICIEA). doi: https://doi.org/10.1109/iciea.2019.8834146
7. Lee, W.-S., Kim, J.-H., Lee, J.-Y., Lee, I.-O. (2019). Design of an Isolated DC/DC Topology With High Efficiency of Over 97% for EV Fast Chargers. IEEE Transactions on Vehicular Technology, 68 (12), 11725–11737. doi: https://doi.org/10.1109/tvt.2019.2949080
8. Helmers, E., Weiss, M. (2017). Advances and critical aspects in the life-cycle assessment of battery electric cars. Energy and Emission Control Technologies, 5, 1–18. doi: https://doi.org/10.2147/eect.s60408
9. Deng, F., Chen, Z. (2015). Voltage-Balancing Method for Modular Multilevel Converters Switched at Grid Frequency. IEEE Transactions on Industrial Electronics, 62 (5), 2835–2847. doi: https://doi.org/10.1109/tie.2014.2362881
10. Plakhtii, O., Nerubatskyi, V., Sushko, D., Ryshchenko, I., Tsybulnyk, V., Hordiienko, D. (2019). Improving energy characteristics of ac electric rolling stock by using the three-level active four-quadrant rectifiers. Eastern-European Journal of Enterprise Technologies, 4 (8 (100)), 6–14. doi: https://doi.org/10.15587/1729-4061.2019.174112
11. Shruti, K. K., Valsalan, T., Poorani, S. (2017). Single phase active front end rectifier system employed in three phase variable frequency drive. International Journal of Innovative Research in Electrical, Electronics, Instrumentation and Control Engineering, 121–129. Available at: https://ijireeice.com/wp-content/uploads/2017/05/IJIREEICE-nCORETech-16.pdf
12. Islam, M. M., Shareef, H., Mohamed, A. (2018). Optimal location and sizing of fast charging stations for electric vehicles by incorporating traffic and power networks. IET Intelligent Transport Systems, 12 (8), 947–957. doi: https://doi.org/10.1049/iet-its.2018.5136
13. Vasiladiotis, M., Rufer, A. (2015). A Modular Multiport Power Electronic Transformer With Integrated Split Battery Energy Storage for Versatile Ultrafast EV Charging Stations. IEEE Transactions on Industrial Electronics, 62 (5), 3213–3222. doi: https://doi.org/10.1109/tie.2014.2367237
14. Bodo, N., Levi, E., Subotic, I., Espina, J., Empringham, L., Johnson, C. M. (2017). Efficiency Evaluation of Fully Integrated On-Board EV Battery Chargers With Nine-Phase Machines. IEEE Transactions on Energy Conversion, 32 (1), 257–266. doi: https://doi.org/10.1109/tec.2016.2606657
15. Huang, Z., Wong, S.-C., Tse, C. K. (2017). Design of a Single-Stage Inductive-Power-Transfer Converter for Efficient EV Battery Charging. IEEE Transactions on Vehicular Technology, 66 (7), 5808–5821. doi: https://doi.org/10.1109/tvt.2016.2631596
16. Kim, D.-H., Kim, M.-J., Lee, B.-K. (2017). An Integrated Battery Charger With High Power Density and Efficiency for Electric Vehicles. IEEE Transactions on Power Electronics, 32 (6), 4553–4565. doi: https://doi.org/10.1109/tpel.2016.2604404
17. Taylor, A., Lu, J., Zhu, L., Bai, K. (Hua), McAmmond, M., Brown, A. (2018). Comparison of SiC MOSFET-based and GaN HEMT-based high-efficiency high-power-density 7.2 kW EV battery chargers. IET Power Electronics, 11 (11), 1849–1857. doi: https://doi.org/10.1049/iet-pel.2017.0467
18. Kwon, M., Jung, S., Choi, S. (2015). A high efficiency bi-directional EV charger with seamless mode transfer for V2G and V2H application. 2015 IEEE Energy Conversion Congress and Exposition (ECCE). doi: https://doi.org/10.1109/ecce.2015.7310418
19. Srdic, S., Lukic, S. (2019). Toward Extreme Fast Charging: Challenges and Opportunities in Directly Connecting to Medium-Voltage Line. IEEE Electrification Magazine, 7 (1), 22–31. doi: https://doi.org/10.1109/mele.2018.2889547
20. Kumari, B., Sankar, M. (2014). Modeling and individual voltage balancing control of modular multilevel cascade converter. International Journal of Emerging Engineering Research and Technology, 2 (1), 42–48.
21. Nerubatskyi, V., Plakhtii, O., Hordiienko, D., Khoruzhevskyi, H. (2019). Simulation of surge protection according IEC 61000-4-5. International scientific journal «Industry 4.0», 4 (6), 293–296.
22. Venkatramanan, D., Bharadwaj, P., Adapa, A. K., John, V. (2019). Power Conversion Technologies for High-Performance AC Micro-grid. INAE Letters, 4 (1), 27–35. doi: https://doi.org/10.1007/s41403-018-00062-6
23. Martinez-Rodrigo, F., Ramirez, D., Rey-Boue, A., de Pablo, S., Herrero-de Lucas, L. (2017). Modular Multilevel Converters: Control and Applications. Energies, 10 (11), 1709. doi: https://doi.org/10.3390/en10111709
24. Nerubatskyi, V. P., Plakhtii, O. A., Karpenko, N. P., Hordiienko, D. A., Tsybulnyk, V. R. (2019). Analysis of energy processes in a seven-level autonomous voltage inverter at various modulation algorithms. Information and control systems on railway transport, 5, 8–18. doi: https://doi.org/10.18664/ikszt.v24i5.181286

25. Mali, S. M., Patil, B. G. (2018). THD Minimization in Multilevel Inverter Using Optimization Approach. International Journal of Engineering Research & Technology (IJERT), 7 (6), 97–100.
26. Sonia, K., Seshadri, G. (2015). Analysis and modelling of a multilevel inverter in distribution system with FACTS capability. International Journal of Innovative Research in Science, Engineering and Technology, 4 (5), 3015–3021.
27. Aghdam, M., Fathi, S., Gharehpetian, G. B. (2008). Harmonic Optimization Techniques in Multi-Level Voltage-Source Inverter with Unequal DC Sources. Journal of Power Electronics, 8 (2), 171–180.
28. Kurwale, M. V., Sharma, P. G., Bacher, G. (2014). Performance analysis of modular multilevel converter (MMC) with continuous and discontinuous pulse width modulation (PWM). International Journal of Advanced Research in Electrical, Electronics and Instrumentation Engineering, 3 (2), 7463–7474. Available at: https://pdfs.semanticscholar.org/d351/b7b2b80426065468fd-39c8d746f70fee1296.pdf
29. Plakhtii, O., Nerubatskyi, V., Karpenko, N., Hordiienko, D., Butova, O., Khoruzhevskyi, H. (2019). Research into energy characteristics of single-phase active four-quadrant rectifiers with the improved hysteresis modulation. Eastern-European Journal of Enterprise Technologies, 5 (8 (101)), 36–44. doi: https://doi.org/10.15587/1729-4061.2019.179205
30. Zhou J., Suand J., Wang X. (2014). Pre-charging control of modular multilevel converter. High Voltage Apparatus, 50 (4), 103–107.
31. Solas, E., Abad, G., Barrena, J. A., Aurtenetxea, S., Carcar, A., Zajac, L. (2013). Modular Multilevel Converter With Different Submodule Concepts – Part I: Capacitor Voltage Balancing Method. IEEE Transactions on Industrial Electronics, 60 (10), 4525–4535. doi: https://doi.org/10.1109/tie.2012.2210378
32. Plakhtii, O. A., Nerubatskyi, V. P., Hordiienko, D. A., Tsybulnyk, V. R. (2019). Analysis of the energy efficiency of a two-level voltage source inverter in the overmodulation mode. Naukovyi Visnyk Natsionalnoho Hirnychoho Universytetu, 4 (172), 68–72. doi: https://doi.org/10.29202/nvngu/2019-4/9
33. Yang, H., Saeedifard, M. (2017). A Capacitor Voltage Balancing Strategy With Minimized AC Circulating Current for the DC–DC Modular Multilevel Converter. IEEE Transactions on Industrial Electronics, 64 (2), 956–965. doi: https://doi.org/10.1109/tie.2016.2613059
34. Plakhtii, O., Nerubatskyi, V., Sushko, D., Hordiienko, D., Khoruzhevskyi, H. (2020). Improving the harmonic composition of output voltage in multilevel inverters under an optimum mode of amplitude modulation. Eastern-European Journal of Enterprise Technologies, 2 (8 (104)), 17–24. doi: https://doi.org/10.15587/1729-4061.2020.200021
35. Kelrykh, M., Fomin, O. (2014). Perspective directions of planning carrying systems of gondolas. Metallurgical and Mining Industry, 6, 64–67.
36. Plakhtii, O., Nerubatskyi, V., Karpenko, N., Ananieva, O., Khoruzhevskyi, H., Kavun, V. (2019). Studying a voltage stabilization algorithm in the cells of a modular sixlevel inverter. Eastern-European Journal of Enterprise Technologies, 6 (8(102)), 19–27. doi: https://doi.org/10.15587/1729-4061.2019.185404
37. Korneliuk, S., Dmitriev, P., Tugay, D. (2019). Empirical support of the mathematical model of the wind turbine WPI. Lighting Engineering & Power Engineering, 2 (55), 68–72. doi: https://doi.org/10.33042/2079-424x-2019-2-55-68-72
38. Bashir, S. B., Beig, A. R. (2018). An improved voltage balancing algorithm for grid connected MMC for medium voltage energy conversion. International Journal of Electrical Power & Energy Systems, 95, 550–560. doi: https://doi.org/10.1016/j.ijepes.2017.09.002
39. Plakhtii, O. A., Nerubatskyi, V. P., Kavun, V. Y., Hordiienko, D. A. (2019). Active single-phase four-quadrant rectifier with improved hysteresis modulation algorithm. Naukovyi Visnyk Natsionalnoho Hirnychoho Universytetu, 5, 93–98. doi: https://doi.org/10.29202/nvngu/2019-5/16
40. Scherback, Y. V., Plakhtiy, O. A., Nerubatskiy, V. P. (2017). Control characteristics of active four-quadrant converter in rectifier and recovery mode. Tekhnichna Elektrodynamika, 6, 26–31. doi: https://doi.org/10.15407/techned2017.06.026
41. Zhemerov, G. G., Krylov, D. S. (2018). Concept of construction of power circuits of a multilevel modular converter and its transistor modules. Electrical Engineering & Electromechanics, 6, 26–32. doi: https://doi.org/10.20998/2074-272x.2018.6.03
42. Franco, V., Zacharopoulou, T., Hammer, J., Schmidt, H., Mock, P., Weiss, M., Samaras, Z. (2016). Evaluation of Exhaust Emissions from Three Diesel-Hybrid Cars and Simulation of After-Treatment Systems for Ultralow Real-World NOx Emissions. Environmental Science & Technology, 50 (23), 13151–13159. doi: https://doi.org/10.1021/acs.est.6b03585
43. Nerubatskyi, V., Plakhtii, O., Kotlyarov, V. (2019). Analysis of topologies of active four-quadrant rectifiers for implementing the INDUSTRY 4.0 principles in traffic power supply systems. International scientific journal «Industry 4.0», 4 (3), 106–109.
44. Plakhtii, O., Nerubatskyi, V., Philipjeva, M., Mashura, A. (2019). Research of mathematical models of lithium-ion storages. International scientific journal «Mathematical modeling», 3 (4), 127–130.
45. Tugay, D., Sayenko, Y., Kolontaevsky, Y., Shkurpela, A. (2019). Distributed solar photovoltaic power station conversion system with power filtration function. International Ukraine-Poland Seminar «Power quality in distribution networks with distributed generation», 131–138. doi: http://doi.org/10.32073/iepl.2019.15
46. Plakhtii, O. A., Nerubatskyi, V. P., Kavun,, A. M., Mashura, A. V. (2018). Compensation of input current harmonics in parallel multiple voltage sourse inverters. Electrical and computer systems, 27 (103), 65–74. doi: https://doi.org/10.15276/eltecs.27.103.2018.07
47. Plakhtii, O. A., Nerubatskyi, V. P., Hordiienko, D. A., Khoruzhevskyi, H. A. (2020). Calculation of static and dynamic losses in power IGBT-transistors by polynomial approximation of basic energy characteristics. Naukovyi Visnyk Natsionalnoho Hirnychoho Universytetu, 2, 82–88. doi: https://doi.org/10.33271/nvngu/2020-82
48. Nerubatskyi, V., Plakhtii, O., Ananieva, O., Zinchenko, O. (2019). Analysis of the Smart Grid concept for DC power supply systems. International scientific journal «INDUSTRY 4.0», 4 (4), 179–182.